Stochastic resonance and self-tuning: A simple threshold system

Takeo Kondo and Toyonori Munakata
Department of Applied Mathematics and Physics, Graduate School of Informatics, Kyoto University, Kyoto 606-8501, Japan
(Received 13 January 2009; revised manuscript received 25 March 2009; published 22 June 2009)

To put it in the framework of information processing, stochastic resonance (SR) is a phenomenon in which the transfer of information from input to output signals can be significantly increased by noise with appropriate (nonzero) intensity. The minimum requirements for SR are generally input signals, nonlinearity, and noise, in addition to a quantifier to measure the efficiency of information transfer. We study a simple threshold system and propose an adaptation mechanism for system parameters, such as a threshold and noise intensity (i.e., temperature), which are held fixed in a normal SR setting. Our emphasis is put on parameter dynamics induced by this adaptation, which we call self-tuning (ST), and on how this dynamics modifies or changes the SR picture with respect to information processing efficiency. As a measure for performance of the threshold system we take mutual information and the signal-to-noise ratio. These quantities are calculated by an analytical method and by a simulational one. ST of temperature results in oscillatory time variation in temperature with its average located around the temperature at which performance is maximized in the SR setting. ST of a threshold turns out to improve performance in the weak noise region.

DOI: 10.1103/PhysRevE.79.061121 PACS number(s): 05.40.−a, 05.10.Gg, 87.10.Vg

I. INTRODUCTION

In some nonlinear systems increasing noise can lead to the formation of more regular temporal and/or spatial structures. Stochastic resonance (SR), which represents one of the salient and ubiquitous examples of this nontrivial behavior, stands for phenomena for which the ordered response of a system to weak input signals can be significantly increased by *selecting* or *tuning* proper noise intensity [1–3].

To be more concrete, let us take a simple threshold system [4,5], with a threshold θ and in contact with a reservoir with temperature T, which produces noises to be fed to the threshold system. If one employs some measure m_{IP} for system performance with respect to information processing (IP), this measure becomes a function of θ and T, which are kept constant during the measurement of $m_{\mathrm{IP}}(\theta,T)$. In the usual SR setting, one pays attention to its T dependence, and SR means that $m_{\mathrm{IP}}(\theta,T)$ for a fixed θ shows a peak structure with its maximum attained at $T^*(\theta)(>0)$ which may generally depend on θ. For convenience we may call T^* the SR temperature.

In this paper we extend a SR model by giving adaptation dynamics to some system parameters, such as θ and/or T and compare m_{IP} for two systems, with and without adaptation dynamics, partly to understand SR itself and partly to search for some mechanisms which may contribute to the improvement of system performance represented by m_{IP}. In developing a model of adaptation, we rely on a feedback mechanism, which we call *self-tuning* (ST) [6,7], by which output signals are fed back to modify system parameters. Originally an idea of ST was developed to explain high sensitivity of auditory systems (hair cells). To describe dynamics here one needs at least three variables, and a limit cycle associated with the Hopf bifurcation plays a decisive role for detection of faint sounds [6].

Although the ST mechanism to be described below is considerably simpler than the ST mechanism proposed for auditory systems [6,7], we will call it ST since there are some points in common between the two mechanisms. That is, choosing θ as a system parameter to be adapted, our ST consists of the processes where the threshold is simply decreasing when there is no firing, i.e., no cross-threshold events and it is raised only if the firing event occurs. In view of the facts that information transfer is effected via firing events in the threshold system, and too small firing rate may be avoided by lowering a threshold, we expect a rather good performance irrespective of current situations of input signals and/or environment (noise source) to which the system is exposed.

The structure of this paper is as follows. In Sec. II we introduce a simple threshold system. After discussing its elementary properties, we discuss SR based on two measures m_{IP}, the mutual information (MI) and the signal-to-noise ratio (SNR) [8].

In Sec. III ST of temperature T, by which T becomes time (n) dependent, i.e., T_n, is considered. Simulation results for time variation in T_n, together with the MI between input and output signals, are presented. We show that T_n fluctuates around the SR temperature T^*, where the maximum of MI is attained.

Next in Sec. IV we introduce a system with two thresholds, one positive and the other negative, which are self-tuned depending on the output from the system. We closely study the dynamics of the thresholds and show that due to ST of the thresholds, MI monotonically decreases as a function of T as in the case of ST for auditory systems [6,7]. Consequently there exists a crossover temperature, T_{cr}, beyond which (i.e., $T>T_{cr}$) ST may result in the deterioration of performance for transfer of information. Section V contains some remarks and conclusion.

II. SR IN THE SIMPLE THRESHOLD SYSTEM

A. Model and measure m_{IP}

We first introduce a simple threshold system with its output y_n at time n given by

$$y_n = \Theta(|s_n + \xi_n| - \theta), \tag{1}$$

where s_n and ξ_n are the input signal and the noise at time n, respectively, and θ denotes the threshold. The function $\Theta(x)$ takes 1(0) when x is positive (negative). Later we will often use the word "firing" when y_n is not zero. The noise ξ_n is assumed to be a zero average Gaussian variable with

$$\langle \xi_n \rangle = 0,$$

$$\langle \xi_n \xi_n' \rangle = T \delta_{n,n'}, \tag{2}$$

where T, to be called temperature, measures the strength of the noise and $\delta_{n,n'}$ stands for the Kronecker delta. Later in Secs. III and IV we introduce the dynamics for T or θ, making these quantities time (i.e., n) dependent.

As a measure m_{IP} for correlation between input $\{s_n\}$ and output signals $\{y_n\}$, we take the mutual information $M(s:y)$ [9], which is expressed as

$$M(s:y) = H_y - H_{y|s}, \tag{3}$$

with H_y and $H_{y|s}$ denoting the Shannon entropies

$$H_y = -\sum_{y=0,1} p(y) \ln p(y),$$

$$H_{y|s} = \int ds p(s) \left[-\sum_{y=0,1} p(y|s) \ln p(y|s) \right]. \tag{4}$$

Here $p(y)$ and $p(s)$ represent the distribution function of $\{y_n\}$ and $\{s_n\}$, respectively, and $p(y|s)$ is the conditional distribution function of y given the input signal s. Since we always indicate the arguments for the function p, no confusion would be incurred due to our use of the same functional symbol p.

For our model, the noise ξ is Gaussian and we have

$$p(1|s) = \{\mathrm{erfc}[(\theta - s)/\sqrt{2T}] + \mathrm{erfc}[(\theta + s)/\sqrt{2T}]\}/2,$$

$$p(0|s) = 1 - p(1|s), \tag{5}$$

where $\mathrm{erfc}(x) = \frac{2}{\sqrt{\pi}} \int_x^\infty dt \exp(-t^2)$. As for the input signal s_n we take a sinusoidal one

$$s_n = A_0 \cos(\omega_0 n \Delta t), \tag{6}$$

which has been widely used [1].

As the input signal s_n is a deterministic function of time n, one may wonder how $p(s)$ could be defined. For the present problem, let us first assume that $t = n\Delta$ is sampled uniformly in the range $-\pi/(2\omega_0) < t < \pi/(2\omega_0)$. Then from the relation $p_{\cos}(s)ds = p(t)dt = dt/(\pi/\omega_0)$, we have

$$p_{\cos}(s) = 1/[\pi \sqrt{A_0^2 - s^2}]. \tag{7}$$

It is noted that Eq. (7) is valid irrespective of the assumed range of uniformity of t [10].

We suppose that important correlations between $\{s_n\}$ and $\{y_n\}$ consists not in ordering of the occurrence of $\{s_n\}$ but in the histogram of the pair $\{s_n, y_n\}$ or $p(y|s)$. $p_{\cos}(y)$ is then given with use of the relation

$$p_{\cos}(y) = \int ds p(y|s) p_{\cos}(s), \tag{8}$$

together with Eqs. (5) and (7). Since we consider only the sinusoidal input, Eq. (6), we will hereafter omit the subscript cos in Eqs. (7) and (8).

At this point we give two remarks. First, a so-called dynamical MI between two dynamical processes $X(t)$ and $Y(t)$ has gathered considerable interest, especially for biological systems [11–13]. For example, a dynamical MI is obtained along the similar lines as path integrals for linear quantum systems [11]. It is also calculated under a Gaussian approximation to study stochastic resonance in the FitzHugh-Nagumo model [12]. A slightly simpler expression for a dynamical MI is employed to study neuronal activity [13].

Second, as will be shown later in Sec. II B (Figs. 2 and 3), $M(s:y)$ calculated in this way, which may be called a static MI, is remarkably similar to the SNR, which takes into account full dynamical information of the input signals. It is also remarked here that accurate numerical calculation of $M(s:y)$ is rather easy, compared with such dynamical quantities as SNR and the dynamical MI mentioned above. We only need to sample the pair (s_n, y_n) from numerical simulations and to calculate the conditional probability $p(y|s)$ as a histogram from the data. This property is especially desirable, as stated in Sec. III B, where we discuss the effects of ST.

We proceed to another measure, the SNR [1,14], which has been playing important roles from an early stage of SR investigation [15]. As we now show, this can be also calculated exactly for model (1). Let us suppose that for the input signals $s(n\Delta t) = A_0 \cos(\omega_0 n \Delta t)$ we have the corresponding output signals $y_n = y(n\Delta t)$.

The time-correlation function ϕ_k is defined by

$$\phi_k = \overline{\langle y_n y_{n+k} \rangle} \quad (k = 0, 1, \ldots, N-1), \tag{9}$$

where the average $\langle \cdots \rangle$ is over the noise ξ_n, ξ_{n+k}, and $\bar{A}_n \equiv (1/N) \Sigma_{n=1}^{n=N-1} A_n$ denotes the average over the time n, which removes the n dependence involved in A_n [14]. (For a discrete time power spectrum, see Chap. 12 of [16].) Since the noise ξ_n $(n = 1, 2, \ldots)$ are independent of each other, Eq. (2), we readily see that

$$\phi_k = \overline{\langle y_n \rangle} \delta_{k,0} + \overline{\langle y_n \rangle \langle y_{n+k} \rangle} (1 - \delta_{k,0}) \equiv g \delta_{k,0} + h_k (1 - \delta_{k,0}), \tag{10}$$

where $\langle y_n \rangle$ is explicitly given in Eq. (5) as

$$\langle y_n \rangle = \{\mathrm{erfc}[(\theta - s_n)/\sqrt{2T}] + \mathrm{erfc}[(\theta + s_n)/\sqrt{2T}]\}/2. \tag{11}$$

In Eq. (11) we see that $\langle y_n \rangle$ is periodic in time $t = n\Delta t$ with the period $t_p = \pi/\omega_0$. This is seen intuitively by observing from Eqs. (1) and (6) that $\langle y_n \rangle$ becomes large when $s_n \simeq \pm 1$, which occurs twice per input signal period $2\pi/\omega_0$. Thus the function h_k itself is also periodic with the period $t_p/\Delta t$. For simplicity we first fix a large integer N and choose Δt to be $\Delta t = t_p/N$. Neglecting higher harmonics which are irrelevant for SNR [1], we have

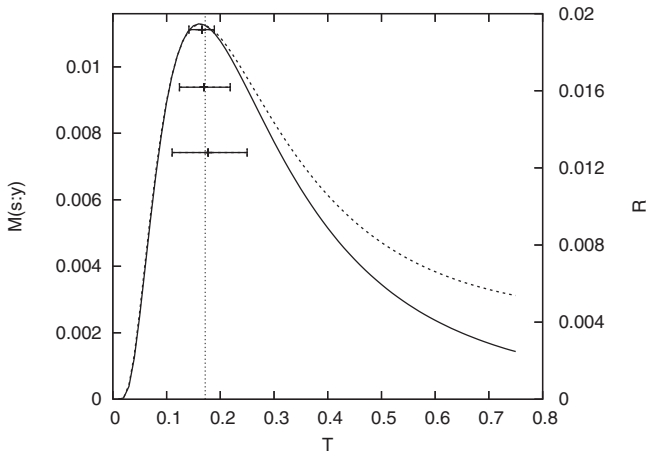

FIG. 1. Mutual information $M(s:y)$ (dotted line) and SNR R (solid line) for the simple threshold system (1) as a function of T. The vertical line is at $T=T^*$ and three horizontal line segments, which we call LS_1, LS_2, and LS_3 from the top, correspond to points P_1, P_2, and P_3 introduced in Sec. III B, respectively.

$$h_k \simeq B\cos(2\pi k/N), \tag{12}$$

with

$$B = (2/N)\sum_{k=0}^{N-1} h_k \cos(2\pi k/N). \tag{13}$$

If we define the power spectrum P_n [16] as

$$P_n = \sum_{k=0}^{N-1} \phi_k \exp[2\pi i k n/N] \quad (n = 0,1,2,\ldots,N-1), \tag{14}$$

we have

$$P_n = g + B(N/2)[\delta_{n,1} + \delta_{n,N-1}] = g + B(N/2)[\delta_{n,1} + \delta_{n,-1}], \tag{15}$$

where we used the fact that P_n is cyclic with period N [16]. From the above we may define SNR, which is notationally expressed as R, by

$$R = B/g. \tag{16}$$

R represents the ratio of the (normalized) power at frequency $2\omega_0$ divided by the noise power g as in the case of continuous time [1]. In passing it is noted that the summation to obtain B [see Eq. (13)] and g, which is necessary for the calculation of R, Eq. (16), is numerically performed by using Eq. (11) to calculate the summands.

B. SR in a threshold system

In Fig. 1 we show $M(s:y)$ and R for $\omega_0=0.5$, $A_0=0.5$, and $\theta=1$ as a function of T. In spite of the apparent difference between $M(s:y)$, Eq. (3), and R, Eq. (16), we observe that $M(s:y)$ behaves quite similarly as R. Each function takes its maximum at $T^* \simeq 0.18$, which demonstrates that the transfer of information through the threshold system (1) is enhanced by proper amount of noise (SR).

$M(s:y)$ and R are shown in Figs. 2 and 3, respectively, as a function of A_0 and T for $\omega_0=0.5$ and $\theta=1$. The similarity between $M(s:y)$ and R, presented in Figs. 1–3, states that SNR is a good quantifier of information transfer. On the other hand, time ordering of the input signals [Eq. (6)] is not crucial to estimate MI between the input and output signals, thus making a static MI based on the assumption, Eq. (7), a good substitute for a dynamic MI [10–12].

III. SELF-TUNING OF TEMPERATURE

A. Temperature dynamics and parameter range

If we have means to control the temperature T of the system and require the best performance on the threshold

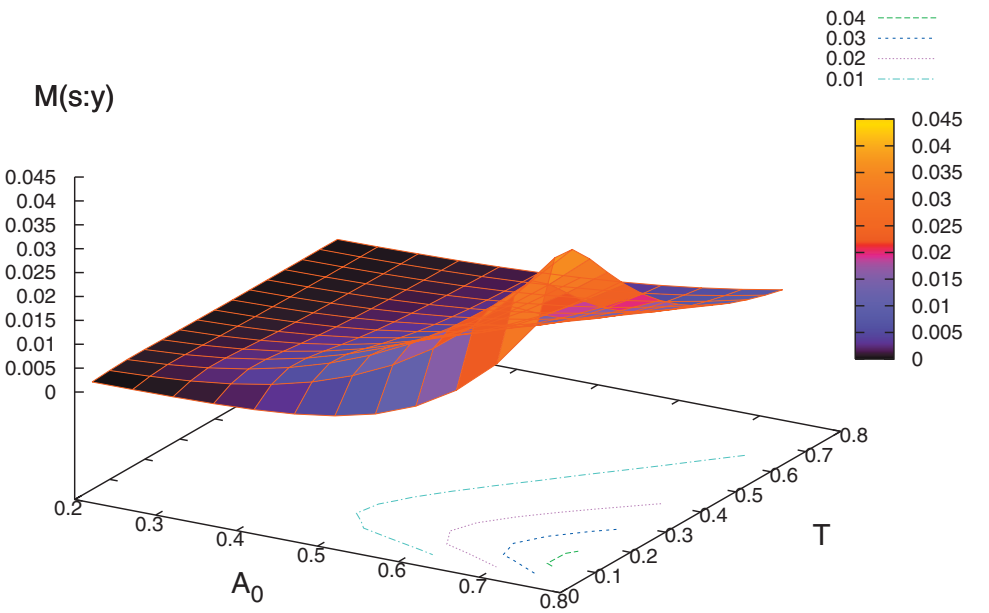

FIG. 2. (Color) Mutual information as a function of A_0 and noise intensity T.

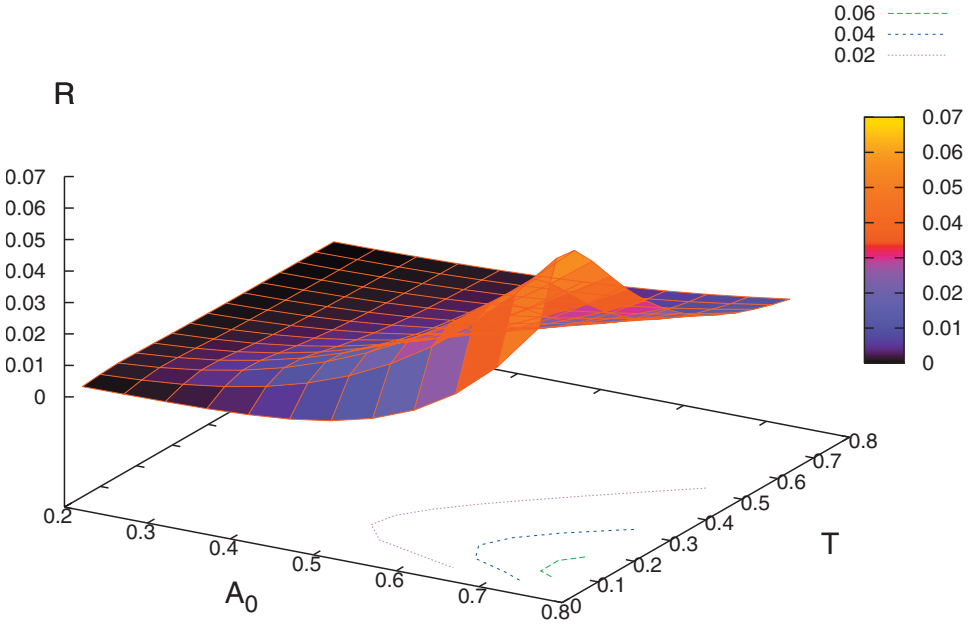

FIG. 3. (Color) R as a function of A_0 and noise intensity T.

system (1), we would set T to be the SR temperature T^*. We now introduce adaptive dynamics for system temperature T, by which T_n (now a function of time n) is expected to behave "efficiently" from a viewpoint of transinformation. From a different viewpoint, we have in mind a thought experiment, in which a movable living unit put in an environment with temperature gradient moves back and forth depending on the output from its neuron. Our results below show that the living unit would be located around the place whose temperature is T^*.

In developing a model for the dynamics of temperature, we try to take into account the feedback of the output y_n on temperature at time $n+1$, T_{n+1}. Here we rely on the idea of ST, which in short means that a parameter, controlling a firing rate of an excitable unit such as a neuron, changes so as to enhance the firing rate if there is no firing event. On the other hand, if there occurs a firing event, the parameter is changed in another direction to avoid too many firing events. (One formulation along this line for neuronal adaptation can be found in [17].)

One simple algorithm which seems to fulfill this requirement employs two-parameter dynamics

$$T_{n+1} = \alpha T_n - \beta y_n \quad (\alpha > 1, \beta > 0), \tag{17}$$

where y_n is obtained from Eq. (1) with T in Eq. (2) replaced by T_n. When $y_n=0$, we expect $T_{n+1} > T_n$ to make firing easier, leading to $\alpha > 1$. When $y_n=1$, we expect $T_{n+1} < T_n$ and β must be positive. Of course there are many other possibilities for the dynamics of T_n and this will be touched upon later (see Sec. V).

The update algorithm (17) with Eq. (1) turns out to be divergent for some parameter range of (α, β) and it is important to have some estimate about the range where convergence is achieved. For the purpose we assume that T_n approaches T_f, which is estimated from

$$T_f = \alpha T_f - \beta \langle y \rangle_{T_f}, \tag{18}$$

where $\langle y \rangle_{T_f} = \int ds p(y=1|s) p(s)$ and $p(s)$ is given by Eq. (7). Equation (18) is now rewritten as

$$(\alpha - 1) T_f / \beta = \langle y \rangle_{T_f}. \tag{19}$$

Plotting both sides of Eq. (19) as a function of T_f we notice that Eq. (19) have three solutions $T_{f,0}=0 < T_{f,1} < T_{f,2}$ if the condition

$$(\alpha - 1)/\beta \leq 0.4 \tag{20}$$

is satisfied. As will be noted later, $\langle T_n \rangle$ oscillates around a stationary value and condition (20) is necessary but not sufficient for algorithm (17) to be convergent. On the other hand, when β gradually becomes large with α fixed, from Eq. (17) we find that T_n approaches zero, which is a stationary solution to both Eqs. (17) and (18). This situation is not reflected in condition (20). That is, we are not interested in the solution $T_f=0$ but Eq. (20) does not exclude this solution. Based on these observations we studied mainly along the line $(\alpha-1)/\beta=0.355$ in the parameter space (α, β). Especially our results are shown for three points, $P_1(\beta=0.005)$, $P_2(\beta=0.01)$, and $P_3(\beta=0.015)$.

B. Analytical and simulational approaches

Let us first consider how T_n changes with time. From Eq. (17) we notice that the ensemble average of T_n (over many runs with the initial condition T_0 fixed) $a_n \equiv E(T_n)$ of T_n evolves in time according to

$$a_{n+1} = \alpha a_n - \beta E(\langle y_n \rangle (T_n)), \tag{21}$$

where $\langle y_n \rangle (T_n)$ is given by Eq. (11) with T replaced by T_n. In order to make Eq. (21) a recursion equation for $\{a_n\}$, we assume $E(\langle y_n \rangle (T_n)) \simeq \langle y_n \rangle (a_n)$, thus leading to

$$a_{n+1} = \alpha a_n - \beta \langle y_n \rangle (a_n), \tag{22}$$

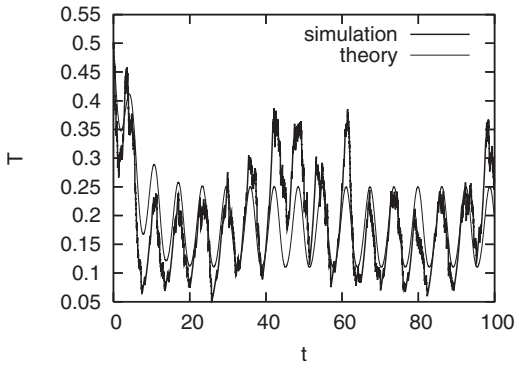

FIG. 4. Temperature dynamics in a transient ($t<30$) state and in a stationary ($t>30$) state, simulation Eq. (17) and theory Eq. (22).

Equation (22) is a more precise description of the temperature evolution than Eq. (18), since the latter cannot capture the oscillation of temperature as shown below. If one specifies $a_0=T_0$, Eq. (22) can be solved to give $a_n=E(T_n)$ uniquely.

We plot in Fig. 4 one realization of the random process $\{T_n\}$ and a_n at an early stage including the transient state ($t<30$) and in a stationary state ($t>30$) for (α,β) corresponding to P_1. It is seen that T_n shows large fluctuations superimposed on oscillatory behavior of a_n with period π/ω_0.

By experiments we numerically obtain $p(y|s)$ by sampling the pair (s_n,y_n) in a stationary state and this yields $M(s:y)$ from Eqs. (3) and (4). In Fig. 1 we plot $M(s:y)$ for three parameter sets represented by P_i $(i=1,2,3)$. Each of the horizontal line segment LS_i $(i=1,2,3)$ in Fig. 1 stands for the center and the amplitude of the oscillation of a_n.

It is first remarked that the averages of temperature for P_i $(i=1,2,3)$ nearly coincide with T^*, shown as a vertical line in Fig. 1. That is, ST seems to bring the temperature T naturally to the optimal one, T^*, a desirable property of ST. This property turns out to be not sensitive to α and β, so long as it is located in the range $0.3\leq(\alpha-1)/\beta\leq0.36$. Second we note that as the amplitude of temperature oscillation increases, $M(s:y)$ decreases, since temperature is sampled from wider range away from the SR temperature T^*.

IV. ST OF THE THRESHOLD

A. Model with two thresholds

Now we turn to ST of a threshold, which is usually held fixed in SR studies. We first modify model (1) by introducing two thresholds, i.e.,

$$y_n=g_{\theta_1,\theta_2}(s_n+\xi_n), \tag{23}$$

where $g_{\theta_1,\theta_2}(x)=1(-1)$ for $x>\theta_1(x<\theta_2)$ and $g_{\theta_1,\theta_2}(x)=0$ for $\theta_2<x<\theta_1$. ξ_n is the Gaussian noise as before, Eq. (2), for the fixed temperature T and the input signal s_n is taken to be Eq. (6) with $A_0=0.5$ and $\omega_0=0.5$.

Naturally the two-threshold system (23) shows SR characteristics for fixed threshold values as will be touched upon in relation to Fig. 6 below. It is noted that the threshold model (23) was recently studied [18] in connection with filtering, where the signal s_n was taken to be the Ornstein-Uhlenbeck process instead of the deterministic one, Eq. (6), and threshold (23) was introduced as an observer of the Brownian motion s_n [18]. In this paper we want to study properties of the system, Eqs. (23) and (24) below more directly without recourse to filtering.

B. Threshold dynamics and mutual information

As in the case of ST of temperature, Eq. (17), we introduce a simple adaptation of θ_1 and θ_2 described by

$$\theta_{1,n+1}=\gamma\theta_{1,n}+F\delta(1,y_n),$$

$$\theta_{2,n+1}=\gamma\theta_{2,n}-F\delta(-1,y_n). \tag{24}$$

F is taken to be a positive constant and γ is $0<\gamma<1$; thus $\theta_{1,n}>0>\theta_{2,n}$ if this relation holds for $n=0$. It is seen in Eq. (24) that $\theta_{1,n}$ decreases and $\theta_{2,n}$ increases if no firing events occur, that is, $y_{n-1}=0$. If, on the other hand, a firing event occurs through $y_{n-1}=1$, which we call $y=1$ firing, $\theta_{1,n}$ is increased by F due to this firing event. Similarly $\theta_{2,n}$ is decreased by F through the $y=-1$ firing event. Through this mechanism we expect and confirm numerically that the threshold values are self-tuned or adjusted to the input signals and noises.

To estimate appropriate values for the two parameters (γ,F), we take the ensemble average of Eq. (24), as we did for Eq. (17), to obtain

$$a_{1,n+1}=\gamma a_{1,n}+Fp_n(1|a_{1,n}),$$

$$a_{2,n+1}=\gamma a_{2,n}-Fp_n(-1|a_{2,n}), \tag{25}$$

where $p_n(1|a_{1,n})$ denotes the probability that $y_n=1$ when the threshold θ_1 is $a_{1,n}$. That is,

$$p_n(1|a_{1,n})=\mathrm{erfc}[(a_{1,n}-s_n)/\sqrt{2T}]/2. \tag{26}$$

Similarly we have $p_n(-1|a_{2,n})=\mathrm{erfc}[(-a_{1,n}+s_n)/\sqrt{2T}]/2$.

In Fig. 5 we plot one realization $(\theta_{1,n},\theta_{2,n})$ and its analytical prediction $(a_{1,n},a_{2,n})$, Eq. (25), for $\gamma=0.95$, $F=0.1$ but for different temperatures, (a) $T=0.03$, (b) $T=0.1$, and (c) $T=0.5$. We see generally that the process $(\theta_{1,n},\theta_{2,n})$ fluctuates around the average $(a_{1,n},a_{2,n})$.

It is noted that when T is low enough [Fig. 5(a)], there occur only $y=1$ (-1) firing events around the top (bottom) of the input sinusoidal signal, Fig. 5(d). This is reflected to the large mutual information $M(s:y)$ as depicted in Fig. 6. On the other hand, for large T [Fig. 5(c)], we observe a lot of $y=-1$ firing events even around the top of the input signal, resulting in small $M(s:y)$. In Fig. 5(b) we see that the behaviors of $(\theta_{1,n},\theta_{2,n})$ are intermediate between those in Figs. 5(a) and 5(c).

In Fig. 6 $M(s:y)$, obtained by collecting samples of pairs (s_n,y_n) as in Sec. III, is plotted as a function of T for the three cases $F=0.05$, $F=0.1$, and $F=0.2$ from the top ($\gamma=0.95$). Also depicted is $M(s:y)$ for system (23) without ST (solid line).

We first note that SR behavior is observed for the two-threshold system (23) (see the solid line in Fig. 6) if ST is not

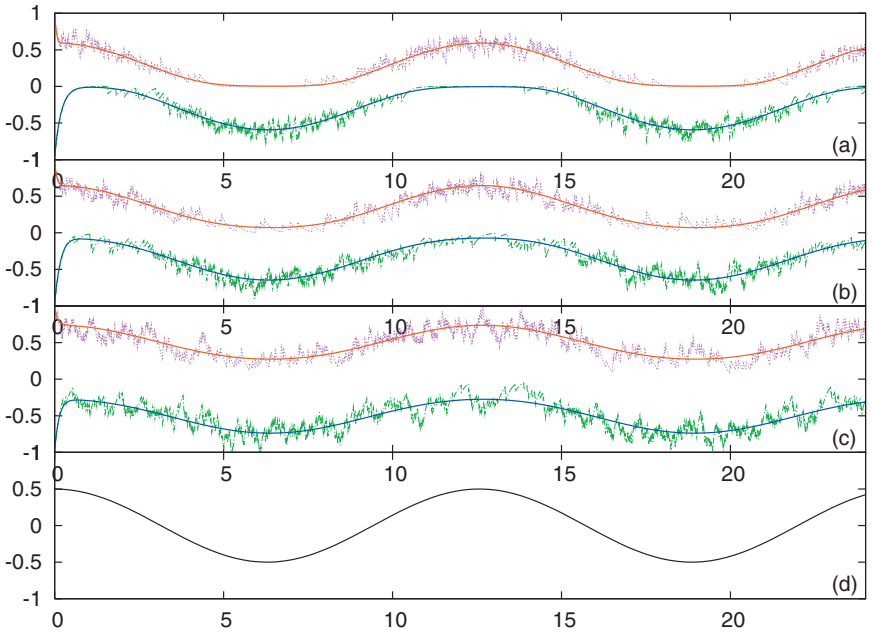

FIG. 5. (Color) θ_1 and θ_2 dynamics as obtained from simulations (θ_1: red lines; θ_2: green lines) and from theory (θ_1: pink lines; θ_2: blue lines) for γ=0.95 and F=0.1. From the top T=0.03, 0.1, and T=0.5. Figure 5(d) depicts the input signal, Eq. (16).

introduced. If F, the size of one-step variation in $\theta_{1,2}$, is large we observe large fluctuations in $\theta_{1,2}$ dynamics (not shown) and the ability of $\theta_{1,2}$ to follow input signals $\{s_n\}$ deteriorates. Reflecting this tendency it is seen in Fig. 6 that $M(s:y)$ decreases as F increases for fixed T. On the other hand, we confirmed numerically that $M(s:y)$ increases monotonically as F is decreased up to 0.001 for fixed T(=0.1). In this connection it is remarked that as F, which may be considered as representing a learning velocity, becomes small, generally one needs longer time for computation to obtain reliable values for $M(s:y)$. This situation is similar to what happens to $M(s:y)$ in Fig. 1. The smaller β in Eq. (17) results in smaller oscillations of T_n and larger $M(s:y)$ but with longer computational time.

Next let us consider the T dependence of $M(s:y)$. As shown in Fig. 5, the ability of $\theta_{1,2}$ to follow input signals $\{s_n\}$ deteriorates as T becomes large, just as in the case of F. More precisely, if we take T=0.03, $\theta_{1,n}(\theta_{2,n})$ nicely follows input signals when it is positive (negative). It is easily seen

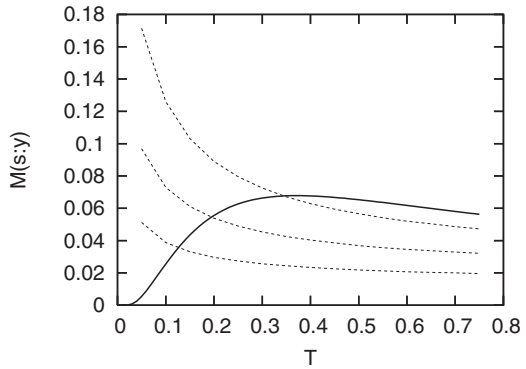

FIG. 6. $M(s:y)$ as a function of T for self-tuned two-threshold system (23) with γ=0.95. The three dotted lines from the top correspond to F=0.05, 0.1 and F=0.2. Also shown is $M(s:y)$ for the two-threshold system (23) with fixed threshold, θ_1=1 and θ_2=−1 (solid line).

that the performance of information processing is enhanced when input signals nearly coincide with the threshold. This explains the general T dependence of the three dotted lines in Fig. 6.

V. SOME REMARKS AND CONCLUSIONS

In concluding this paper we briefly comment on simultaneous ST of T and θ. Let us introduce ST to system (1). For T adaptation we tentatively take Eq. (17) and for θ adaptation we choose Eq. (24) (suitably modified for the one threshold case), resulting in ST represented by

$$T_{n+1} = \alpha T_n - \beta y_n \quad (\alpha > 1, \beta > 0),$$

$$\theta_{n+1} = \gamma \theta_n + F y_n \quad (0 < \gamma < 1, F > 0). \tag{27}$$

A simulation study on Eq. (27) soon revealed that it is rather unstable and T diverges or crosses the physical region $T > 0$. These properties can be traced to the T dynamics in Eq. (27). It is noted that the first term on the right-hand side (rhs) of this equation contributes to increasing T. When T_n becomes large, increment $T_{n+1} - T_n$ can be large and the second term can only have minor effects to compensate this increment; thus T_n easily goes to ∞. When T becomes small, on the contrary the first term on the rhs of Eq. (27) has small effects compared with the second one and it is seen that T_n crosses zero.

This instability could be avoided in Sec. III since we fixed the threshold. Now that we allow time change in the threshold, it turned out to be very difficult to find parameters in Eq. (27) which give physical solution for $\{T_n, \theta_n\}$.

With this observation we modified Eq. (27) to

$$T_{n+1} = \alpha T_n + \beta(1 - y_n) \quad (0 < \alpha < 1, \beta > 0),$$

$$\theta_{n+1} = \gamma \theta_n + F y_n \quad (0 < \gamma < 1, F > 0), \tag{28}$$

which removes the instability mentioned above. Taking ensemble average of Eq. (28) we can derive as before the fol-

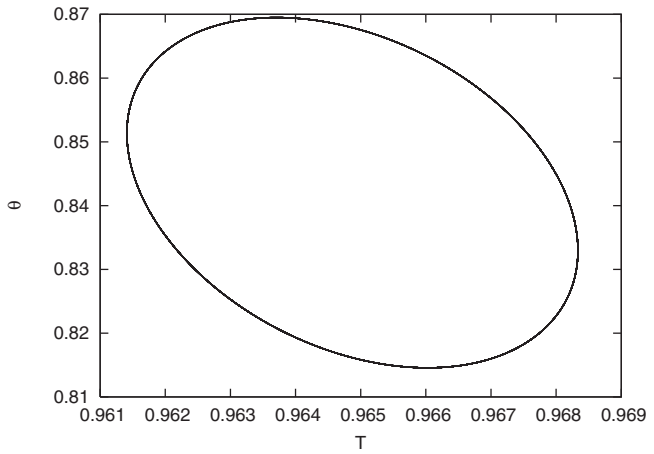

FIG. 7. A limit cycle from Eq. (29) for $(\gamma,F)=(0.95,0.1)$ and $(\alpha,\beta)=(0.995,0.002)$.

lowing equation for $a_{1_n}\equiv E(T_n)$ and $a_{2,n}\equiv E(\theta_n)$:

$$a_{1,n+1}=\alpha a_{1,n}+\beta[1-\langle y_n\rangle(a_{1,n},a_{2,n})],$$

$$a_{2,n+1}=\gamma a_{2,n}+F\langle y_n\rangle(a_{1,n},a_{2,n}), \tag{29}$$

with $\langle y_n\rangle(a_{1,n},a_{2,n})$ given by Eq. (11) with θ and T replaced by $a_{2,n}$ and $a_{1,n}$, respectively. We confirmed numerically that $(a_{1,n},a_{2,n})$ as $n\to\infty$ is attracted to a limit cycle.

Since the set of ST Eq. (28) contains four parameters, we fixed $(\gamma,F)=(0.95,0.1)$, which was used in Sec. IV for threshold self-tuning. Tentatively setting $(\alpha=0.995,\beta=0.002)$ we show in Fig. 7 the limit cycle produced by the map dynamics (29). This is a typical limit cycle we found by solving Eq. (29). For a given T we have two θ and the ellipse leans with negative gradient (correlation). Thus when T is large θ can be smaller, as compared with the case when T is small. This (negative) correlation is expected to result in larger firing rate (time average firing rate 0.42 with ST and 0.35 without ST), and consequently larger $M(s:y)$ compared with the case of no ST.

To confirm this aspects of ST we fixed $(\gamma,F)=(0.95,0.1)$. For each of the three β values, $\beta_1=0.0015$ (blue circles), $\beta_2=0.002$ (green circles), and $\beta_3=0.0025$ (red circles) we took 20 α values from 0.99 to 0.9995 with the width 0.0005. In Fig. 8 we plot $M(s:y)$, which is obtained by simulations as in Secs. III and IV, for (α,β_i) $(i=1,2,3)$ as a function of (time) averaged temperature T. For the sake of comparison $M(s:y)$ without ST for $\theta=1$ (full curve) is also plotted as a full curve in Fig. 8.

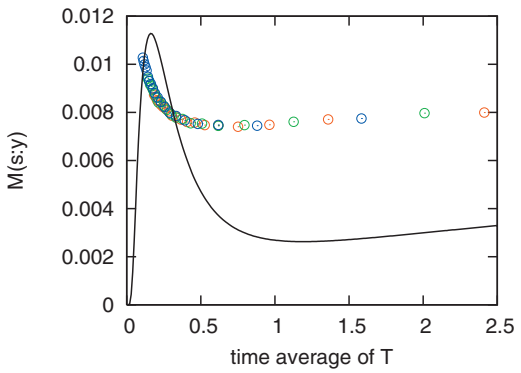

FIG. 8. (Color) $M(s:y)$ as a function of (time averaged) temperature with ST based on Eq. (28). For $(\gamma,F)=(0.95,0.1)$ fixed, and for $\beta=0.002$ we chose 20 α values and corresponding $M(s:y)$ are plotted with green circles. (From left to right α values are increasing.) For $\beta=0.0025$ (red) and $\beta=0.0015$ (blue) $M(s:y)$ are also plotted. For comparison $M(s:y)$ with no ST $(\theta=1)$ is shown as a full curve.

We notice that the overall performance of ST is good, especially when an average T is slightly larger than the SR temperature, T^*. In this T region firing rate (on average) was found to be increased by about 1/4 of the case without ST.

Our studies on simultaneous ST of both T and θ is rather limited but suggest some potential utility of a limit cycle, which realizes "negative" correlation between T and θ, desirable for efficient information transfer. However, we have to mention that the parameters used to define the dynamics of the ST mechanism, which appear in Eq. (27) and also in Eqs. (17) and (24), had to be tuned or chosen properly. This issue may diminish the practical application of the ST mechanism proposed in this work.

ACKNOWLEDGMENTS

One of the authors (T.M.) would like to thank Takahiro Hada, Boyoung Seo, Raishma Krishnan, and Michio Ueda for helpful discussions during research work on SR. This work was supported by a Grant-in-Aid from the Ministry of Education, Culture, Science and Technology of Japan.

[1] L. Gammaitoni, P. Haenggi, P. Jung, and F. Marchasoni, Rev. Mod. Phys. **70**, 223 (1998).
[2] T. Wellens, V. Shatokhin, and A. Buchleitner, Rep. Prog. Phys. **67**, 45 (2004).
[3] V. S. Anishchenko, V. V. Astakhov, A. B. Neiman, T. E. Vadivasova, and L. Schimansky-Geier, *Nonlinear Dynamics of Chaotic and Stochastic Systems* (Springer, Berlin, 2002).
[4] Z. Gingl, L. B. Kiss, and F. Moss, EPL **29**, 191 (1995).
[5] L. Gammaitoni, Phys. Lett. A **208**, 315 (1995).
[6] W. Denk, W. W. Webb, and A. J. Hudspeth, Proc. Natl. Acad. Sci. U.S.A. **86**, 5371 (1989); S. Camalet, T. Duke, F. Juelicher, and J. Prost, *ibid.* **97**, 3183 (2000).
[7] J. F. Lindner, M. Bennett, and K. Wiesenfeld, Phys. Rev. E **72**, 051911 (2005).
[8] L. B. Kish, G. P. Harmer, and D. Abbott, Fluct. Noise Lett. **1**, L13 (2001).
[9] T. M. Cover and J. A. Thomas, *Elements of Information Theory* (Wiley, New York, 1991).
[10] R. A. Wannamaker, S. P. Lipshitz, and J. Vanderkooy, Phys. Rev. E **61**, 233 (2000).

[11] I. Goychuk and P. Haenggi, New J. Phys. **1**, 14 (1999).
[12] T. Munakata and M. Kamiyabu, Eur. Phys. J. B **53**, 239 (2006).
[13] J. K. Douglass, L. Willkins, E. Pantazelou, and F. Moss, Nature (London) **365**, 337 (1993); J. E. Levin and J. P. Miller, *ibid.* **380**, 165 (1996); W. Bialek, M. De Veese, F. Rieke, and D. Warland, Physica A **200**, 581 (1993).
[14] B. McNamara and K. Wiesenfeld, Phys. Rev. A **39**, 4854 (1989).
[15] R. Benzi, S. Sutera, and V. Vulpiani, J. Phys. A **14**, L453 (1981).
[16] W. H. Press, B. P. Flannery, S. A. Teukolsky, and W. T. Vetterling, *Numerical Recipes in C* (Cambridge University Press, Cambridge, England, 1988).
[17] T. Toyoizumi, J.-P. Pfister, K. Aihara, and W. Gerstner, Proc. Natl. Acad. Sci. U.S.A. **102**, 5239 (2005).
[18] T. Munakata, T. Hada, and M. Ueda, Physica A **375**, 492 (2007).